Thermal Stability and Reducibility of Oxygen-Containing Functional Groups on Multiwalled Carbon Nanotube Surfaces: A Quantitative High-Resolution XPS and TPD/TPR Study

Shankhamala Kundu, Yuemin Wang, Wei Xia, and Martin Muhler*

Laboratory of Industrial Chemistry, Ruhr-University Bochum, D-44780 Bochum, Germany

Received: May 19, 2008; Revised Manuscript Received: August 8, 2008

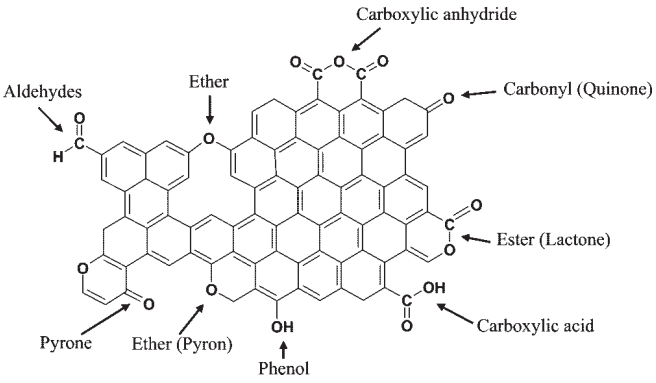
The thermal stability and the reducibility of oxygen-containing functional groups on the surface of nitric acid-treated multiwalled carbon nanotubes (CNTs) have been studied using temperature-programmed desorption and reduction (TPD and TPR) and high-resolution X-ray photoelectron spectroscopy (XPS). The thermal treatments up to 720 °C were carried out in the XPS setup, either under ultrahigh vacuum (UHV) or in diluted hydrogen. Deconvoluted XP spectra were used for the quantitative determination of the amount of the different functional groups on the CNT surfaces as a function of the pretreatment. The number of the oxygen atoms per unit surface area was obtained from the oxygen to carbon (O/C) ratio derived from the corresponding peak areas in the XP spectra. The results obtained by XPS agree quantitatively with the observations by TPD and TPR. The acid treatment not only introduced carboxyl, carbonyl, and phenol groups on the surface but also generated ether-type oxygen groups between the graphitic layers as indicated by the oxygen balance. Generally, the presence of hydrogen decreased the thermal stability of the oxygen-containing functional groups. Both XPS and TPR provided evidence for the reduction of carboxylic groups to phenolic groups at 300 °C in hydrogen. Heating in hydrogen was found to be more effective in removing the oxygen-containing functional groups compared to heating in UHV but did not allow either to remove all oxygen species even at 720 °C.

Downloaded via UNIV AT BUFFALO STATE UNIV NEW YORK on March 5, 2025 at 23:27:41 (UTC).
See https://pubs.acs.org/sharingguidelines for options on how to legitimately share published articles.

1. Introduction

Because of their unique texture and properties such as superior electrical conductivity and mechanical stability, carbon nanotubes (CNTs) have become one of the most promising materials in various fields of applications.[1−4] In the field of heterogeneous catalysis, attention is being focused on multiwalled CNTs as support due to their excellent mechanical and chemical stability and their high thermal and electrical conductivity.[5,6] Like graphite, CNTs are hydrophobic and inert in nature, and it is therefore difficult to achieve a high dispersion of metal particles on CNTs. Treatment of CNTs with oxidizing agents in the gas or liquid phase results in partial surface oxidation, that is, the formation of surface oxygen-containing functional groups, which can be acidic or basic in nature.[7−9] Nitric acid or other oxidizing media such as ozone or oxygen plasma have been reported to be highly effective for this purpose.[10−14] It has been shown that the basal planes of the graphite are attacked by molecular oxygen only at their periphery or at defect sites such as edge planes and vacancies.[15−17] Toebes et al.[18] reported that in nitric acid the nitronium ion (NO_2^+) is able to attack aromatic compounds, which is probably the first step for the generation of the oxygen containing functional groups. After oxidation, the CNT surfaces have hydrophilic properties, which enhances the wettability for polar solvents. Moreover, the oxygen functional groups can be used as anchoring sites for the immobilization of metal particles and large molecules.[19,20] Therefore, the detailed knowledge of the nature and amount of oxygen functional groups on the CNT surfaces is of great interest, especially for using CNTs as catalyst support.

SCHEME 1: Schematic Representation of Oxygen Functional Groups Present on the Carbon Nanotube Surface



The nature and concentration of surface functional groups can be modified by thermal treatments. Heating in inert atmosphere may be used to selectively remove some of these functional groups. The type and the amount of the oxygen functional groups depend on the oxidizing agents. Scheme 1 shows several functional groups on CNT surfaces after nitric acid treatment.[18−21] Carboxyls, carboxylic anhydrides, and lactones are generally present. Hydroxyl groups at the edge of the graphitic planes exhibit phenolic character. Carbonyl groups can remain isolated like quinones, or they can be arranged like pyrones. Furthermore, the ether-type oxygen or pyran can substitute one carbon atom at the edge. Finally, aldehydes can also be present on the surface of the oxidized CNTs.

A variety of experimental techniques has been used up to now to identify the oxygen functional groups present on oxidized

* To whom correspondence should be addressed. Tel: +49 234 32 28754. Fax: +49 234 32 14115. E-mail: muhler@techem.rub.de.

10.1021/jp804413a CCC: $40.75 © 2008 American Chemical Society
Published on Web 10/02/2008

MRD EX. 2030
LGES v MRD
IPR2024-01011

CNTs, such as acid−base titration,[7,8,16,22] infrared spectroscopy (IR),[19,21,23,24] X-ray photoelectron spectroscopy (XPS),[21,25−27] and temperature-programmed desorption (TPD).[19,20,28,29] However, the identification of the nature and the determination of the amount of oxygen functional groups remains a challenge due to their complexity.

Boehm et al.[7,8] used the titration method to determine the total oxygen content and the type of functional groups. In contact with the aqueous solutions with different pH values, negatively, neutral, and positively charged surface sites can be formed on CNT surfaces. However, this method is limited by the fact that it failed to account for a large amount of the total oxygen content on the carbon surface.[16,29] Ros et al.[19] employed IR and thermogravimetry-mass spectroscopy (TG-MS) and showed that the surface oxidation of CNTs in the liquid phase proceeds via carbonyl groups followed by the conversion into carboxylic groups and carboxylic anhydrides. Park et al.[30] identified the oxygen functional groups such as C═O (1710 cm^{-1}), C−O (1300 cm^{-1}), and OH (3450 cm^{-1}) by means of IR spectroscopy. FTIR can only be used for highly oxidized carbon surfaces, otherwise the intensity of the absorption bands is very poor. Diffuse reflectance IR spectroscopy (DRIFTS) is preferable to avoid the problems caused by sample dilution. However, the interpretation of the spectra is complicated, because each band can include contributions from various functional groups,[23] and it is essentially impossible to perform a quantitative analysis of these data.

TPD has been reported as one of the most commonly used techniques to identify the surface functional groups on CNTs, which decompose at different temperatures releasing CO, CO_2, and water. There are some inconsistencies in literature with respect to the assignment of the TPD peaks to specific surface groups, as the peak temperature may be shifted due to the differences in sample mass, heating rate, gas-flow rate, and the reactor dimensions of the experimental set-ups.[19,18,31] However, a specific temperature range can be defined for particular functional groups in general.

Okpalugo et al.[25] showed that high-resolution XPS is an excellent tool to identify the oxygen-containing functional groups, and also tried to quantify the amount of oxygen. In another study, Lakshminarayanan et al.[26] investigated the relative percentage of different oxygen functional groups from the deconvoluted XP spectra. Toebes et al.[18] reported the amount and the thermal stability of the oxygen functional groups in inert atmosphere by combined thermogravimetry, acid−base titration, and XPS measurements. However, the thermal stability of these oxygen surface groups in hydrogen has not yet been studied in detail.

Here, we report on the thermal stability of oxygen-containing surface groups on CNTs both in UHV and in reducing atmosphere investigated by TPD, TPR, and high-resolution XPS. The amount and the type of oxygen functional groups were identified, and the transformation of these groups upon heating to high temperature in UHV and in hydrogen was studied. The number of oxygen atoms per unit surface area was derived from the XPS-based O/C ratio and compared with the quantitative results obtained from the TPD and TPR experiments.

2. Experimental Section

Multiwalled CNTs with inner diameters of 20−50 nm and outer diameters of 70−200 nm were obtained from Applied Sciences Inc. (Ohio, USA). These CNTs consist of concentric graphene sheets parallel to the structure axis. The as-received CNTs were first thermally treated under flowing helium for 1 h at 800 °C to remove the polyaromatic impurities on the surface. The thermally treated CNTs were then refluxed in boiling nitric acid (65%) for 90 min. After cooling, the CNTs were filtered and washed with distilled water until pH 7. The CNTs were finally dried at 100 °C for 16 h.

The TPD and TPR experiments with the oxidized CNTs were carried out in a flow setup operating at atmospheric pressure in helium and in a mixture of helium and hydrogen, respectively. The gas composition leaving the reactor was monitored via a quartz capillary by an online mass spectrometer (MS, Omnistar, Pfeiffer), which was calibrated for He, H_2, CO, CO_2, NO, and H_2O to determine quantitatively the gas species evolved during the TPD and TPR. Argon was used as internal standard, and zero-gas calibration was performed before each calibration and also before each measurement to obtain a reliable background. The following high-purity gas mixtures were used for calibration: 5.04% He in Ar, 4.09% H_2 in Ar, 9.98% CO in Ar, 1.05% CO_2 in Ar, and 3133 ppm NO in Ar. The calibration of water was achieved by passing He (10 sccm) through three saturators, filled with distilled water, in series kept at 0 °C. The calibration factors obtained for all the gases were then verified by introducing known amount of gas mixtures. In a typical measurement, 200 mg of the oxidized CNTs were loaded into a tubular quartz reactor with an inner diameter of 20 mm. The CNTs were first dried at 80 °C for 60 min in flowing helium. Subsequently, the CNTs were heated under He at a flow rate of 50 sccm with a heating ramp of 10 K min^{-1}, and TPD profiles of CO, CO_2, H_2O, and NO were monitored by the online MS. In case of TPR, a gas mixture of H_2 and He (1:9, total flow 80 sccm) was used. TPR profiles of H_2, H_2O, CO, NO, and CO_2 were obtained at a heating rate of 10 K/min. Both experiments were repeated several times to verify the reproducibility of the data.

XPS measurements were carried out in an ultrahigh vacuum (UHV) setup equipped with a high-resolution Gammadata-Scienta SES 2002 analyzer. A monochromatic Al Kα X-ray source (1486.6 eV; anode operating at 14 kV and 55 mA) was used as incident radiation. The base pressure in the measurement chamber was around 2×10^{-10} mbar. XP spectra were recorded in the fixed transmission mode. The analyzer slit width was set to 0.3 mm and a pass energy of 200 eV was chosen, resulting in an overall energy resolution better than 0.5 eV. Charging effects were compensated by applying a flood gun. The binding energies were calibrated based on the graphite C 1s peak at 284.5 eV. The thermal treatment of the oxidized CNTs in UHV (1×10^{-9} mbar) was carried out in the preparation chamber of the XPS setup for 30 min at 300, 440, 590, and 720 °C, respectively. The treatment under H_2 at around 5 mbar was performed in the reaction chamber of the XPS setup at 300, 440, and 590 °C for 30 min. Because of experimental limitations, prolonged treatment for 120 min at 590 °C was performed instead of 30 min at 720 °C. It was observed that treating the sample at 590 °C for 30 min in H_2 resulted in a strong decrease in the oxygen amount from 13.7 to 2.0%. Prolonged treatment for 2 h at 590 °C in H_2 led to a further decrease of the oxygen content to 1.5%. Hence, only the results obtained after treating the sample for 2 h in H_2 at 590 °C are presented and discussed in the following. The hydrogen-treated samples were then transferred in UHV to the measurement chamber. Prior to individual elemental scans, a survey scan was taken for all the samples to detect all of the elements present.

The CASA XPS program with a Gaussian−Lorentzian mix function and Shirley background subtraction was employed to deconvolute the XP spectra. The fwhm values were fixed at a

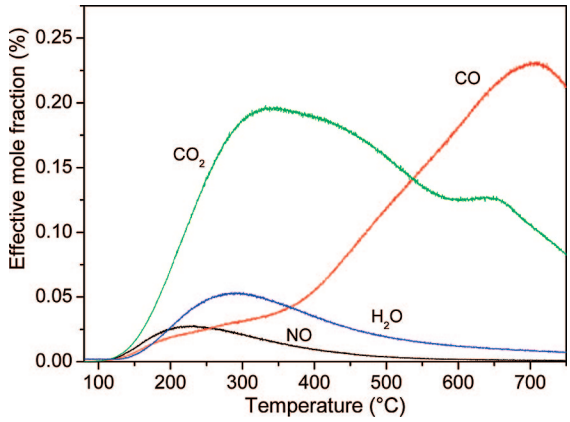


Figure 1. TPD profiles of HNO_3-treated CNTs in helium at a heating rate of 10 K min^{-1}.

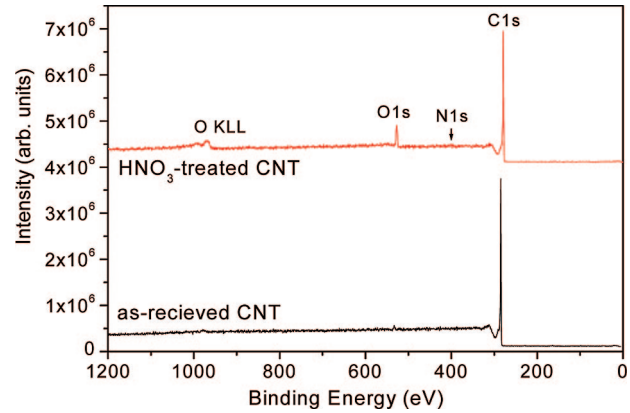


Figure 2. XPS survey scans of as-received and HNO_3-treated CNTs before the thermal treatment in UHV.

maximum limit of 1.5 eV for all of the peaks during the fitting procedure. The peak positions were reproducible along with the fixed Lorentz to Gaussian ratio and fwhm. Care was taken that all the fitting results are self-consistent, so that the corresponding deconvoluted peaks can be compared quantitatively.

The O/C ratio obtained from the XPS measurement was converted to the number of oxygen atoms per unit surface area. The model used for the calculations is mainly based on two assumptions: first, the inelastic mean free paths (λ) of the oxygen and carbon 1s electrons are equal, that is, $\lambda = 3$ nm.[32] Because the interlayer spacing of graphite layer is 0.335 nm, one inelastic mean free path comprises nine consecutive graphite layers. The second assumption is that the thickness of one monolayer of oxygen atoms on the CNT surface is $\lambda/9$. An areal density of carbon atoms of 38.3 nm^{-2} based on the ideal graphite structure is used for the calculations.

The physisorption measurements were carried out with a Quantachrome Autosorb-1-MP system. The BET surface area was determined by static nitrogen physisorption at 77 K subsequent to outgassing at 573 K, until the pressure was lower than 5 mbar.

3. Results

3.1. Thermal Stability in Helium or UHV. The HNO_3-treated CNTs (90 min at 110 °C) were first studied by TPD experiments in helium. Figure 1 shows the TPD profiles of released CO, CO_2, H_2O, and NO obtained upon heating from 80 to 750 °C at 10 K min^{-1}. It can be seen that CO and CO_2 are the major gases evolved. Additional drying at 80 °C before the TPD measurement removed the physisorbed water during sample transfer, as evidenced by the corresponding H_2O peak (not shown). The broad H_2O peak ranging from 150 to 450 °C with a maximum at around 280 °C can be mainly assigned to the formation of carboxylic anhydrides from the dehydration of adjacent carboxyl groups. Another possible source of this water peak could be the dehydration of phenolic hydroxyl groups. The first CO_2 peak evolved at around 340 °C can be attributed to the decomposition of carboxylic groups. The shoulder at about 470 °C and the peak at around 650 °C in the CO_2 profile are believed to be associated with the decomposition of carboxylic anhydrides and lactones, respectively, which are more stable than carboxyl groups. The CO profile shows a dominant peak at 700 °C with additional contributions at lower temperatures of around 470 and 280 °C. The shoulder at 280 °C could be attributed to the decomposition of the ketone or aldehyde groups. The decomposition of carboxylic anhydrides also leads to the release of CO, which appears at around 470 °C similar to CO_2. The CO peak at 700 °C is associated with the decomposition of phenol, quinone, and ether groups, whereas the decomposition of pyrones occurs at even higher temperatures.[19,18,28,30] The generation of CO and CO_2 in different but well defined temperature ranges indicates the presence of chemically different oxygen-containing functional groups on the CNT surfaces.

On the basis of the information obtained from TPD, the oxygen-containing functional groups were further characterized by XPS after thermal treatments at different temperatures. The XPS survey scan shows the elements present on the CNT surfaces (Figure 2). Carbon and oxygen were detected both in the as-received and the acid treated samples. However, the O 1s peak increased significantly after nitric acid treatment. Furthermore, an additional peak appeared at about 400 eV after the nitric acid treatment, indicating the presence of nitrogen-containing species. Impurities were not detected on the sample surfaces.

There is general agreement in literature on the assignment of the peaks in the C 1s, O 1s and N 1s spectra.[21,25−27] Part a of Figure 3 shows the C 1s spectrum of the oxidized CNTs, which can be deconvoluted into the following bands: carbon in graphite at 284.5 eV, carbon singly bound to oxygen in phenols and ethers (i.e., C−O) at 286.1 eV, carbon doubly bound to oxygen in ketones and quinones (i.e., C═O) at 287.5 eV, carbon bound to two oxygens in carboxyls, carboxylic anhydrides, and esters (i.e., −COO) at 288.7 eV, and the characteristic shakeup line of carbon in aromatic compounds at 290.5 eV ($\pi-\pi^*$ transition). The deconvolution of the O 1s spectrum results in two peaks (part b of Figure 3): oxygen doubly bound to carbon (i.e., O═C) in quinones, ketones, and aldehydes at 531.6 eV, and oxygen singly bound to carbon (i.e., O−C) in ethers and phenols at 533.2 eV. Because oxygen atoms in esters, carboxyls, anhydrides, and pyrones have both single bonds and double bonds with carbon atoms, the oxygen atoms in these groups contribute to both the above-mentioned two peaks. As shown in part c of Figure 3, deconvolution of the N 1s spectrum results in two peaks at 400.9 and 406.7 eV, which can be attributed to the nitrogen atoms bound to carbon (i.e., N−C) and to oxygen (i.e., N−O), respectively.

To gain more insight into the thermal stability of these functional groups, XPS measurements of the CNTs after heat treatments at different temperatures were performed. After peak fittings based on these assignments, relative changes of different peak areas can be observed, corresponding to the transformations of different surface functional groups. Figure 4 shows the deconvoluted C 1s spectra, where the intensity variations of the

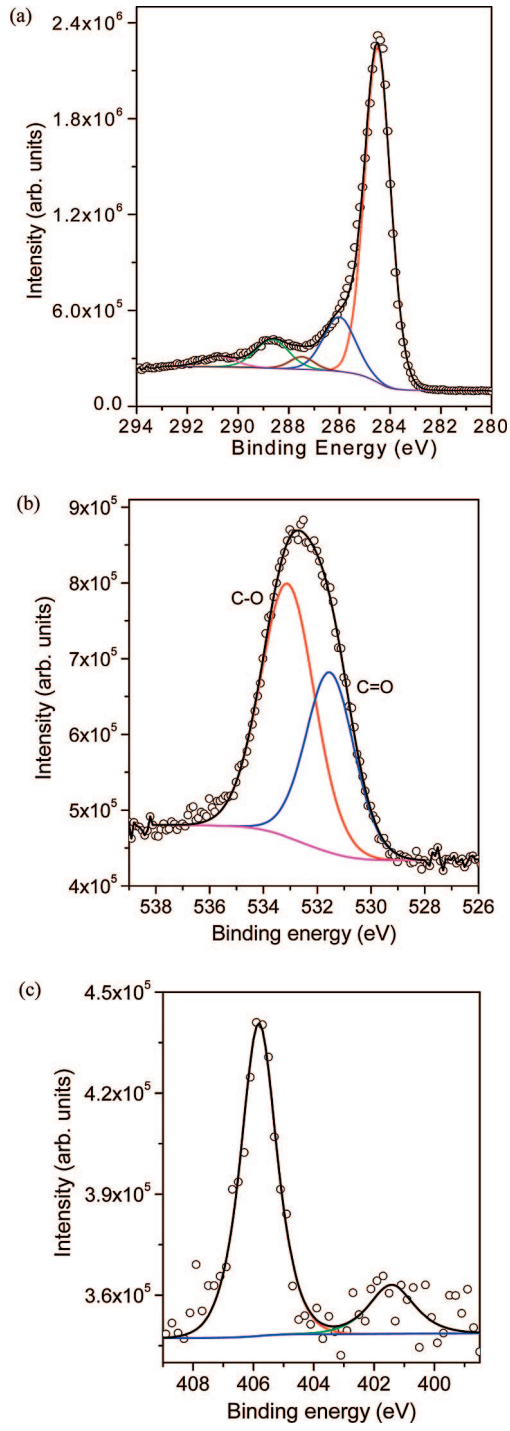


Figure 3. Deconvoluted XP spectra of the (a) C 1s region, (b) O 1s region, and (c) N 1s region obtained with HNO_3-treated CNTs before a thermal treatment in UHV.

derived peaks are clearly visible after heat treatments. The relative concentration of the corresponding functional groups were derived and summarized in Table 1. The amount of graphitic carbon increases upon heating as a result of the decomposition of oxygen- and nitrogen-containing surface functional groups. It can be seen that the functional groups with C−O bonds (phenols, ethers, etc.) are the dominant species on the oxidized CNTs. The second major species are −COO (carboxyls, anhydrides, esters, etc.), which are nevertheless less stable in comparison with other species, as can be seen from the strong decrease of their concentrations with increasing temperature. The groups with C═O bonds (carbonyls, quinones, etc.) are found to be present with the lowest amount as compared to other species at room temperature.

On the basis of the deconvoluted XP C 1s spectra, the atomic ratio of different functional groups to graphitic carbon is plotted and shown in Figure 5. The −COO functional groups decrease significantly after heat treatment at 300 °C, which is mainly due to the decomposition of the carboxylic groups. At the same time, a decrease of the C−O contribution is observed, which can be attributed to the dehydration of adjacent phenolic groups forming water. The change of the C═O peak upon heating to 300 °C appears to be mainly due to the decomposition of aldehyde groups. The −COO groups decrease further rapidly until 590 °C, which can be attributed to the decomposition of the carboxylic anhydrides and ester groups. The TPD results also show pronounced CO_2 and CO peaks in this temperature range. The gradual change of the C−O and C═O spectra between 300 and 600 °C indicates that the decomposition of phenol and pyrone groups already started in this temperature range. After heating to 720 °C, a strong decrease of C−O and C═O is observed indicating the decomposition of ether and quinone groups at high temperatures. The residual −COO groups are believed to be mainly lactones.

Figure 6 presents the deconvoluted XP O 1s spectra of the oxidized CNTs after heat treatment at different temperatures. Fitting of the spectra gives two peaks corresponding to singly and doubly bound oxygen. As discussed above, −COOR contributes to both peaks. At room temperature, more single-bond species are found (60.8%) as derived from the peak areas. The intensities of both the single- and double-bond peaks decrease after heating to 300 °C, which can be attributed to the decomposition of carboxyl groups in this temperature range. Further heating to 590 °C leads to continuous decreases of both peaks with little changes of their area ratios. It is known that mainly the carboxylic anhydrides and ester groups decompose in this temperature range, resulting in the decrease of both C−O and C═O peaks simultaneously. Finally, after heating at 720 °C, the area of the double-bond peak is larger than the single-bond peak (38.7%), which indicates that the single-bond groups are less stable than the double-bond groups at high temperatures. Therefore, although the general trend is the decrease of all oxygen species upon heating, their relative amount is different. These features are in agreement with the results obtained from C 1s spectra and the TPD observations.

The surface atomic concentrations of C, O, and N on the oxidized CNTs are calculated from the corresponding peak areas of the XP spectra (Table 2). The concentration of oxygen increases with a factor of 6 from 1.8 to 10.7% due to the HNO_3 treatment. Additionally, the treatment also introduces around 2% of nitrogen to the CNT surface. It can be seen that both the oxygen and the nitrogen concentrations decrease with increasing treatment temperatures. After heating at 720 °C in UHV, the oxygen concentration on the CNT surface decreases to 4.3%, which is nevertheless still much higher than that of the CNTs before HNO_3 oxidation (1.8%). After thermal treatment at 720 °C in UHV, the rest is believed to be mainly ether-, carbonyl-, and lactone-type oxygen, which were reported to decompose in the range of 700 to 980 °C.[28,31] However, it is shown in the next section that they can decompose at lower temperatures in hydrogen.

3.2. Thermal Stability in Hydrogen. For comparison with the inert atmosphere (helium or UHV), the HNO_3-oxidized CNTs (90 min at 120 °C) were also studied in TPR measurements using diluted hydrogen. The TPR profile in Figure 7 shows that H_2O is the most abundant gas evolved upon heating,

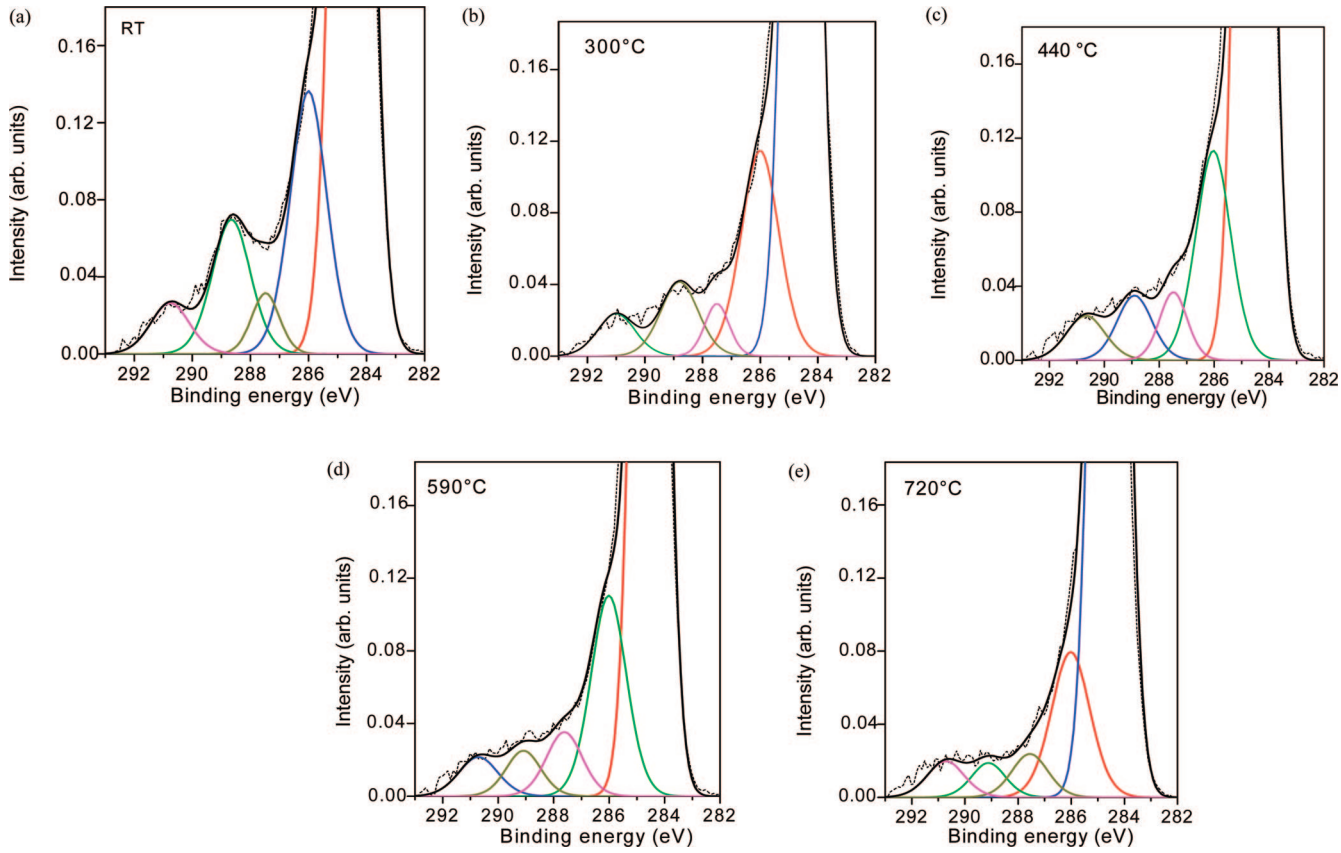


Figure 4. XP C 1s deconvoluted spectra of oxidized CNTs with different pretreatment temperatures in UHV: (a) room temperature (RT), (b) 300 °C, (c) 440 °C, (d) 590 °C, (e) 720 °C.

TABLE 1: Relative Content of Functional Groups Presents in XP C 1s Spectra of Oxidized CNTs after Pretreatment at Different Temperatures in UHV

pre treatment temperature	relative atomic concentrations (%)			
	peak I[a]	peak II[b]	peak III[c]	peak IV[d]
RT	77.6	12.7	4.3	5.4
300	78.3	13.2	3.9	4.6
440	81.4	11.2	3.4	4.0
590	81.8	11.0	4.3	2.9
720	85.4	9.2	3.1	2.3

[a] 284.5 eV: graphitic carbon. [b] 286.1 eV: C−O (phenol, pyran, ether or alcoholic hydroxyls). [c] 287.5 eV: C═O (carbonyl, quinone). [d] 288.3 eV: −COO (carboxyl, carboxyl anhydride, ester).

other than CO and CO_2 in the TPD measurement. The contribution of physisorbed water can be largely excluded due to drying before the TPR measurement. The overall profile of CO_2 in the TPR experiment is similar to that of the TPD experiment in helium. The CO_2 peak evolved at 325 °C corresponds to the decomposition of carboxylic groups. The release of CO_2 at 430 °C and higher temperatures is presumably associated with the decomposition of carboxylic anhydrides and lactones. However, more CO_2 is detected in TPR (0.145%) than in TPD (0.125%) at higher temperatures of about 650 °C. At high temperatures in H_2, both the amount of desorbed CO in the gas phase and the concentration of the active surface complexes, which release CO upon decomposition, are at their maximum,[33] which can therefore enhance the probability of the following secondary Boudouard-type reaction:

$$CO_{gas} + C(O)_{surface} = CO_2 + C_{free} \quad (1)$$

The reaction could be the source of the excess amount of CO_2 at higher temperatures in TPR compared to TPD. Two H_2

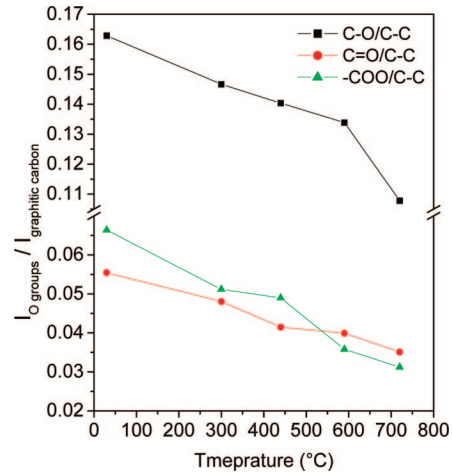


Figure 5. Variation of the atomic ratio of different functional groups to the graphitic carbon after pretreatments at different temperatures in UHV.

consumption peaks were detected in the TPR experiment. The first one, a relatively small peak in the range of 150 to 500 °C with a minimum at around 250 °C, can be attributed to the partial reduction of the carboxylic groups to phenolic groups accompanied by the release of water. It has been reported that the carboxylic anhydride groups are not directly reduced by H_2,[34] which is also confirmed here by the evolution of CO_2 and CO peak at about 430 °C. The carboxylic anhydrides are present at two adjacent dangling carbon sites. It is believed that hydrogen attacks either of the two surface carbon atoms and forces the anhydride complex to form the orientation with minimum potential energy.[34] Finally, it weakens the bond between the dangling carbon atom and the surface carbon atom, resulting

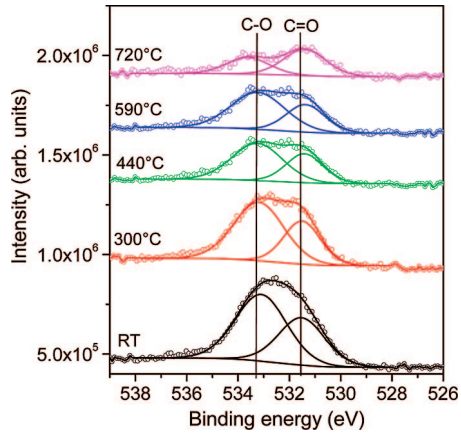


Figure 6. XP O 1s deconvoluted spectra of oxidized CNTs with different pretreatment temperatures in UHV: (a) room temperature (RT), (b) 300 °C, (c) 440 °C, (d) 590 °C, (e) 720 °C.

TABLE 2: XPS Surface Atomic Concentrations[a] of C, O, and N of HNO_3-Treated CNTs (90 min at 110°C) after Pretreatment at Different Temperatures in UHV

pretreatment temperature (°)	C%	O%	N%	O atoms/nm^2
RT	87.0	10.7	2.3	41
300 °C	88.7	8.6	2.7	33
440 °C	90.9	6.6	2.5	25
590 °C	92.3	5.9	1.8	22
720 °C	94.9	4.3	0.8	15

[a] Sensitivity factors, carbon 0.25, oxygen 0.66, nitrogen 0.42.[38]

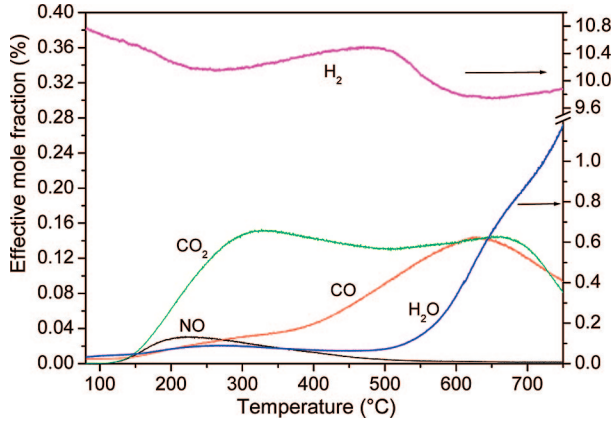


Figure 7. TPR spectra of HNO_3-treated CNTs at a heating rate of 10 K min^{-1} in diluted hydrogen.

in the desorption of carboxylic anhydride groups at relatively lower temperatures (430 °C) than in the absence of hydrogen (470 °C).

Furthermore, the water profiles of the TPD and TPR experiments are quite different. The water amount is higher in TPR (about 0.08%) in the range of 210 to 500 °C in comparison with the TPD profile (about 0.05%). The water evolved at around 250 °C is tentatively assigned to the dehydration of neighboring carboxylic groups with the formation of a carboxylic anhydride group. Water formation at relatively high temperatures (>400 °C) could be assigned to the direct reduction of the aldehyde groups and phenolic hydroxyl groups, which also contribute to the first hydrogen consumption peak. The CO desorption step located at relatively low temperatures of about 280 °C is associated with the decomposition of aldehydes similar to that in TPD. Carboxylic anhydrides decompose into CO and CO_2 at around 430 °C. The CO profile shows a maximum at 650 °C. In hydrogen, a fraction of the CO-containing complexes (mainly quinones and semiquinone-type functional groups) can be directly reduced to H_2O giving rise to the intense water peak at higher temperatures. The surface groups can also be desorbed as CO resulting in the peak around 650 °C. The selectivity depends on the heating rate, and it has been reported that lower heating rates favor the conversion of a large fraction of these surface groups to water-evolving complexes.

Above 600 °C, the H_2 profile shows a strong consumption peak until the final temperature of 750 °C, which is in good agreement with literature.[34] The TPR profile exhibits a sharp increase of the water signal in the high temperature region, whereas a decrease of CO is observed in TPR as compared to the TPD profile. Moreover, the CO peak in the TPR profile shows a clear shift toward lower temperatures. It is known that the release of CO at higher temperatures can be partially attributed to the readsorption of CO at free active sites created after the desorption of surface functional groups at lower temperatures.[33,35] However, in the presence of H_2 the active sites can also interact with H_2. When the chemisorption of H_2 is energetically more preferable over CO, then CO is released at relatively lower temperatures in TPR than in TPD. Because there is less (or no) CO readsorption at lower temperatures, the amount of CO evolved at higher temperature is much lower during TPR.

The effect of H_2 on the thermal stability of the oxygen functional groups on the CNT surface was also studied by high resolution XPS. Survey scans were found to be similar to those shown in Figure 2. The C 1s spectra obtained after thermal treatments in H_2 (5 mbar) are shown in Figure 8. It can be seen that all the deconvoluted peaks corresponding to different functional groups decrease in intensity upon heating. On the basis of the deconvolution, the atomic concentrations of different functional groups were derived and are summarized in Table 3. The deconvoluted spectra show that the relative percentage of the phenol and ether groups is much higher (about 12.9%) and hence are the major species on CNTs before heat treatment, similar to the sample heat-treated in UHV. In comparison with the treatment in UHV, the evolution of the surface groups upon heating appears different in H_2 atmosphere, reflecting the effect of H_2 on the thermal stability of the functional groups.

The atomic ratio of functional groups to the graphitic carbon was plotted against the heating temperature in Figure 9. After heating to 300 °C in H_2, we can see a clear increase of the C−O peak, which can be assigned to the reduction of the carboxylic groups leading to the formation of the phenolic groups. At the same time, carboxyl groups decompose in this temperature range giving rise to a sharp decrease in the −COO peak. Furthermore, a stronger decrease of −COO groups is evident in H_2 (from 6.8 to 5.5%, a decrease of 19%) than in UHV (from 5.4 to 4.6%, a decrease of 15%). These findings support the hypothesis that the carboxyl groups are reduced to phenol groups in this temperature range. The decrease of carbonyl groups can also be attributed to the formation of phenol groups in H_2. All of these results lead to a significant rise of the amount of C−O, which is in good agreement with the TPR observations.

The carboxylic anhydride and lactone groups are known to decompose at relatively high temperatures, which causes a further decreases of −COO groups after heating to 440 and 590 °C (Figure 9). There is a sharp decrease of the amount of C−O groups at 440 °C. One possible reason might be the reduction of phenol groups by H_2 leading to the formation of water. A higher amount of water desorption was also observed in TPR

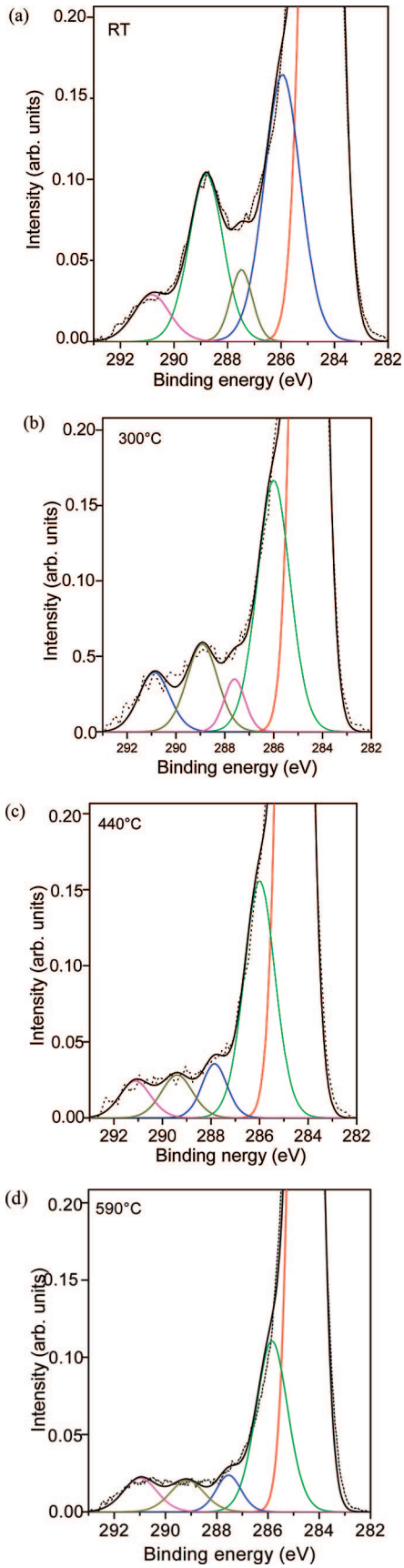


Figure 8. XPS C 1s peak deconvolution of oxidized CNTs after pretreatments in H_2 at different temperatures: (a) room temperature (RT), (b) 300 °C, (c) 440 °C, (d) 590 °C.

in the same temperature range. The C═O groups decreased significantly, when the sample was heated at 590 °C for 2 h in

TABLE 3: Relative Content of Functional Groups Present in XP C1s Spectra of Oxidized CNTs after Pretreatment at Different Temperatures in Hydrogen

pretreatment temperature	relative atomic concentrations (%)			
	peak I[a]	peak II[b]	peak III[c]	peak IV[d]
RT	75.7	12.9	4.6	6.8
300	74.2	16.7	3.6	5.5
440	79.4	14.3	3.3	3.0
590	91.4	5.7	1.5	1.4

[a] 284.5 eV: graphitic carbon. [b] 286.1 eV: C−O (phenol, pyran, ether or alcoholic hydroxyls). [c] 287.5 eV: C═O (carbonyl, quinone). [d] 288.3 eV: −COO (carboxyl, carboxyl anhydride, ester).

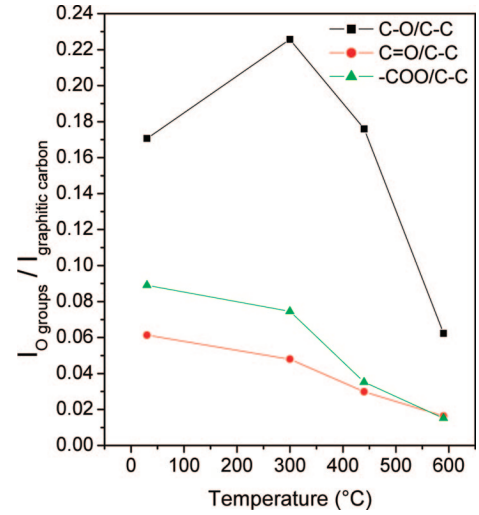


Figure 9. Variation of the atomic ratio of different functional groups to the graphitic carbon after pretreatment at different temperatures in hydrogen.

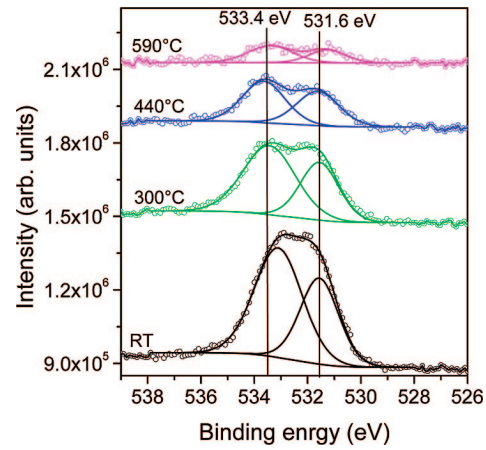


Figure 10. XP O 1s spectra of oxidized CNTs after pretreatment in hydrogen at different temperatures: (a) room temperature (RT), (b) 300 °C, (c) 440 °C, (d) 590 °C.

H_2, which can be assigned to the decomposition of quinone groups. At the same time, a drastic decrease of the C−O groups was observed due to the decomposition of the phenol and ether groups, in good agreement with the TPR results.

The O 1s spectra of the oxidized CNTs after heat treatment in H_2 are shown in Figure 10. At room temperature, the concentration of O−C is higher (61.3% of the total peak area) than that of the O═C (38.7%). With increasing heat treatment temperature, the total intensity of oxygen decreases gradually. Only traces are left after heating to 590 °C under H_2 for 2 h. However, a significant change of the O−C to O═C ratio was

TABLE 4: XPS Surface Atomic Concentrations[a] of C, O, and N of HNO_3-Treated CNTs (90 min at 120°C) after Pretreatment at Different Temperatures in Hydrogen

pretreatment temperature (°C)	C%	O%	N%	O atoms/nm^2
RT	83.9	13.7	2.4	55
300	88.1	9.3	2.6	36
440	92.4	5.8	1.8	21
590	97.5	1.5	1.0	5

[a] Sensitivity factors, carbon 0.25, oxygen 0.66, nitrogen 0.42.[38]

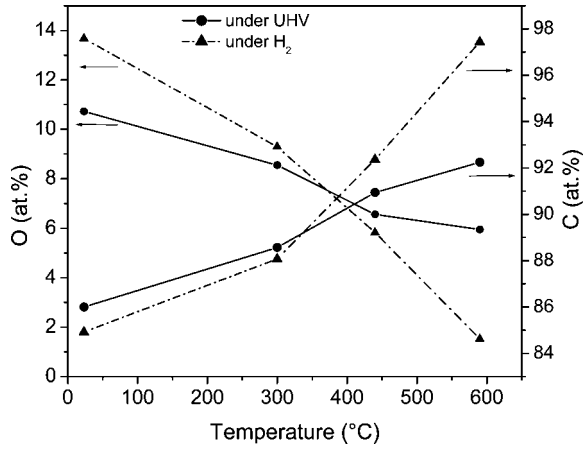


Figure 11. Variation of the XPS-derived composition of functionalized CNTs after pretreatment in UHV and H_2 at different temperatures.

not detected throughout the whole temperature series. The decrease in the O 1s peak intensity at 300 and 440 °C in H_2 can be mainly attributed to the decomposition of carboxyl, carboxylic anhydride, and ester groups. Treatment at 590 °C in H_2 for 30 min leads to further decrease of both oxygen peaks (spectra not shown). A further strong decrease of both peaks was observed after 120 min at 590 °C, which is mainly associated with the decomposition of the phenol, ether, and carbonyl groups in H_2.

The surface atomic concentrations of C, O, and N are summarized in Table 4 as a function of the thermal treatment temperatures. The oxygen concentration increases from 1.8% of the untreated CNTs to 13.7% after the acid treatment. Because of the different temperatures (110 vs 120 °C) applied during the HNO_3 treatment of the CNT samples, the batch treated at higher temperatures had a higher initial oxygen concentration. After heating at 590 °C for 120 min in H_2, the surface oxygen concentration decreases to 1.5%, as compared to 4.3% after treatment for 30 min at 720 °C in UHV. The comparison between the treatments in UHV and H_2 is shown in Figure 11. The surface oxygen concentration is even lower than that of the untreated CNTs, although HNO_3 treatment can introduce surface defects, which are active sites for the binding of oxygen species. Hence, it can be concluded that in H_2 atmosphere the oxygen functional groups are less stable and can decompose or be reduced at lower temperatures.

3. Number of Oxygen Atoms Present on the CNT Surfaces. From the TPD profile, it is possible to quantify the amount of different gases evolved during the desorption process. From the physisorption measurement the BET surface area of the untreated CNT is determined to be about 45 m^2/g, which increases to 64 m^2/g after the acid treatment. Hence, we can calculate the amount of oxygen atoms present on the CNT surface by considering the oxygen atoms present in the CO, CO_2, and H_2O molecules. At the same time, we assume that the detected oxygen functional groups are present only at the surface of the graphite layer, not underneath the graphite layers. The concentration of the oxygen atoms removed from the oxidized CNT surface is derived to amount to 2.87 mmol/g, that is, 27 atom/nm,^{2} obtained from the desorption spectra in helium by solving the mass balance. From the O/C ratio derived from the XP spectra, we can also calculate the concentration of the oxygen atoms present on the surface. The O/C ratio of the untreated CNTs is 0.0175, which corresponds to a value of 6 oxygen atoms/nm.^{2} For the acid-treated CNTs without heat treatment, a value of 41 atoms/nm^2 was estimated, whereas after the thermal treatment at 720 °C under UHV the amount of the surface oxygen atoms decreased to 15 atoms/nm^2. Hence, the amount of the oxygen atoms desorbed in this temperature range was 26 atoms/nm^2 in good agreement with the quantitative TPD results.

Similarly, from the TPR profile the concentration of surface oxygen on the CNTs heated in hydrogen was calculated amount to 6.23 mmol/g, that is, about 58 atoms/nm.^{2} The fact that the amount of the oxygen atoms present on the surface exceeds that of the surface carbon atoms indicates clearly that more ether groups are present underneath the topmost carbon layer. On the basis of this assumption and considering the percentage of different functional groups obtained from the C 1s spectra, we can derive the O/C ratio which is about 0.167. The O/C value obtained from the XPS measurements is 0.163 in good agreement with the theoretically calculated value.

4. Discussion

The HNO_3 oxidation of CNTs introduces a significant amount of oxygen functional groups on the surface and also increases the BET surface area. The TPD studies show that the decomposition of carboxyl, carboxylic anhydride, and ester groups mainly releases CO_2, whereas the decomposition of phenol, ether, and quinone groups leads to CO. The combination of thermal treatment and high-resolution XPS gives more details on the type and thermal stability of the surface functional groups. It was found that H_2 has a pronounced influence on the surface oxygen functional groups interacting with them in different ways depending upon their chemical nature. On the one hand, H_2 reduces some of the surface functional groups directly resulting in the decomposition of these groups and the formation of water. It also destabilizes the surface complexes by attacking the carbon atoms that anchor them to the surface. Additionally, H_2 can occupy the active sites created upon the desorption of the oxygen functional groups by chemisorption, blocking them for the readsorption of gas-phase species.

On the basis of the TPR, TPD, and XPS results, it can be seen that H_2 has a strong influence on the thermal stability of the surface functional groups. The reduction of carboxyls to the phenols by H_2 is supported by both the TPR and XPS results. The intensity of the CO_2 peak evolved at around 340 °C, which is mainly attributed to the decomposition of carboxylic group, is lower (0.151%) in comparison to the CO_2 peak in the TPD experiment (0.196%), that is, in H_2 a smaller amount of carboxyls decompose into CO_2 than in inert gas. Furthermore, a significant increase of the C−O concentration (12.9 to 16.7% in TPR as compared to 12.7 to 13.2% in TPD) is obtained by XPS after heating at 300 °C in H_2, which can be attributed to the formation of phenolic groups. Additionally, a major part of the CO-releasing functional groups, mainly the quinones and the phenols, are directly reduced by H_2 to H_2O, which is evidenced by the significant increase of the water peak and the lower amount of CO evolved during the TPR profile at higher

temperatures (>600 °C). Carboxylic anhydrides are not directly reduced by H_2, but the interaction of these groups with H_2 leads to their destabilization and final desorption at lower temperatures than those in the absence of H_2. As a final point, the presence of H_2 influences readsorption by blocking the active site created due to the desorption of surface functional groups. These active sites are then hydrogen-terminated and cannot anchor other species. Without H_2, CO and other species play the same role resulting in the partial regeneration of surface functional groups. All of the above results indicate that H_2 has a significant influence on the thermal stability of the surface oxygen functional groups and can be used as a probe molecule to identify the functional groups on the CNT surfaces.

For the quantification of the surface oxygen concentration, the frequently employed titration method failed to detect a large amount of oxygen sites.[16] Thus, the oxygen concentration determined by other methods are always higher. [7,8,31,36] It has been suggested that, in addition to the oxygen atoms bound at the edge planes, ether links between the adjacent carbon layers are very likely present.[19] These hidden atoms are not accessible for titration, also not for TPD or TPR to some extent due to the higher desorption energy of ether, but accessible for XPS. This is verified by our TPD, TPR, and XPS studies, in which a general agreement is established on the desorbing amount of oxygen species obtained from these methods. The total amount of oxygen atoms on CNTs was found to be 41 atoms/nm^2 based on the XPS studies. It is actually not possible that all these atoms are on the outermost surface because the oxygen content exceeds the number of the exposed carbon atoms. Mawhinney et al.[37] found that only about 4% of the carbon atoms of SWNT were bound to the oxygen atoms introduced by acid treatment. The percentage could be higher in case of multiwalled CNTs due to the presence of surface defects. However, there is no doubt that a large amount of oxygen atoms is located subsurface, which is also confirmed by the XPS studies, where the deconvolution of the C 1s spectra shows that the concentration of C−O groups is rather high. The embedded oxygen atoms are relatively stable but can still be released upon heating, especially in the presence of H_2. After treatment for 120 min in H_2 at 590 °C, the oxygen concentration is even lower than that of the untreated CNTs, although the nitric acid treatment can introduce surface defects, which are active sites for the binding of oxygen species. Finally, the surface is assumed to be largely terminated by C−H after this treatment and is therefore fully inert.

5. Conclusions

The different oxygen functional groups on CNT surfaces were quantitatively identified by XPS. In addition to carboxyl, carbonyl, and phenol groups, ether-type oxygen between the two adjacent graphite layers was found to be created by the nitric acid treatment. The deconvoluted XP spectra allow the quantitative determination of different oxygen species on the CNTs after thermal treatment at different temperatures. It was found that the decomposition of the carboxylic groups occurs in the lower temperatures range, whereas the phenol, ether, and carbonyl groups are more stable and decompose at higher temperatures. After heating to 720 °C in UHV, the concentration of surface oxygen atoms decreases from 10.7 to 4.3%, revealing that the functional groups cannot be completely removed under these conditions.

The comparison of the results obtained in UHV and H_2 reveals that H_2 has a marked influence on the thermal stability of the surface functional groups. The functional groups can be removed by direct reduction (carboxyl, phenol, quinone, carbonyl, etc.), or through destabilization of their anchoring to the carbon surface (anhydride, etc.) in the presence of H_2. Both XPS and TPR provided evidence for the reduction of carboxylic groups to phenolic groups at 300 °C in hydrogen. Generally, a clear decrease of decomposition temperatures in H_2 was demonstrated for different functional groups. The amount of oxygen species reached a lower value (1.5%) after treatment in H_2 than in UHV (4.3%) and even than the untreated CNTs (1.8%), despite the presence of surface defects introduced by the nitric acid treatment. The CNTs in this stage are assumed to be largely C−H terminated, with a small amount of oxygen atoms left between the graphite layers in form of ether-type groups.

Acknowledgment. S. Kundu thanks the International Max Planck Research School *Surface and Interface Engineering in Advanced Materials* (SurMat) for a research grant.

References and Notes

(1) Baughman, R. H.; Zakhidov, A. A.; de Heer, W. A. *Science* **2002**, *297*, 787.

(2) Mestl, G.; Maksimova, N. I.; Keller, N.; Roddatis, V. V.; Schloegl, R. *Angew. Chem., Int. Ed.* **2001**, *40*, 2006.

(3) Delgado, J. J.; Vieira, R.; Rebmann, G.; Su, D. S.; Keller, N.; Ledoux, M. J.; Schlögl, R. *Carbon* **2006**, *44*, 809.

(4) Tessonnier, J. P.; Pesant, L.; Ehret, G.; Ledoux, M. J.; Pham-Huu, C. *Appl. Catal., A* **2005**, *288*, 203.

(5) de Jong, K. P.; Geus, J. W. *Catal. Rev.-Sci. Eng.* **2000**, *42*, 481.

(6) Auer, E.; Freund, A.; Pietsch, J.; Tacke, T. *Appl. Catal., A* **1998**, *173*, 259.

(7) Boehm, H. P. *Carbon* **1994**, *32*, 759.

(8) Boehm, H. P. *Carbon* **2002**, *40*, 145.

(9) Barton, S. S.; Evans, M. J. B.; Halliop, E.; Macdonald, J. A. F. *Carbon* **1997**, *35*, 1361.

(10) Ajayan, P. M.; Ebbesen, T. W.; Ichihashi, T.; Ijima, S.; Tanigaki, T.; Hiura, H. *Nature* **1993**, *362*, 522.

(11) Kooi, S. E.; Schlecht, U.; Burghard, M.; Kern, K. *Angew Chem. Int. Ed.* **2002**, *41*, 1353.

(12) Hiura, H.; Ebbesen, T. W.; Tanigaki, T. *Adv. Mater.* **1995**, *7*, 275.

(13) Banerjee, S.; Hemraj-Benny, T.; Wong, S. S. *Adv. Mater.* **2005**, *17*, 17.

(14) Klein, K. L.; Melechko, A. V.; McKnight, T. E.; Retterer, S. T.; Rack, P. D.; Fowlkes, J. D.; Joy, D. C.; Simpson, M. L. *J. Appl. Phys.* **2008**, *103*, 061301/1.

(15) Radovic L. R. *Chemistry and Physics of Carbon*, Marcel Dekker Inc., New York, 2003.

(16) Boehm, H. P. *Adv. Catal.* **1966**, *16*, 179.

(17) Anderson J. R. *Structure of Metallic Catalysts*; Academic Press Inc.: U.S., 1975.

(18) Toebes, M. L.; van Heeswijk, J. M. P.; Bitter, J. H.; van Dillen, A. J.; de Jong, K. P. *Carbon* **2004**, *42*, 307.

(19) Ros, T. G.; van Dillen, A. J.; Geus, J. W.; Koningsberger, D. C. *Chem.—Eur. J.* **2002**, *8*, 1151.

(20) Xia, W.; Su, D.; Birkner, A.; Ruppel, L.; Wang, Y.; Woell; Qian, J.; Liang, C.; Marginean, G.; Brandle, W.; Muhler, M. *Chem. Mater.* **2005**, *17*, 5737.

(21) Martinez, M. T.; Callejas, M. A.; Benito, A. M.; Cochet, M.; Seeger, T.; Anson, A.; Schreiber, J.; Gardon, C.; Marhic, C.; Chauvet, O.; Fierro, J. L. G.; Maser, W. K. *Carbon* **2003**, *41*, 2247.

(22) Jagiello, J.; Bandosz, T. J.; Schwarz, J. A. *Carbon* **1994**, *32*, 1026.

(23) Fanning, P. E.; Vannice, M. A. *Carbon* **1993**, *31*, 721.

(24) Kastner, J.; Pichler, T.; Kuzmany, H.; Curran, S.; Blau, W.; Weldon, D. N. *Chem. Phys. Lett.* **1994**, *221*, 53.

(25) Okpalugo, T. I. T.; Papakonstantinou, P.; Murphy, H.; McLaughlin, J.; Brown, N. M. D. *Carbon* **2005**, *43*, 153.

(26) Lakshminarayanan, P. V.; Toghiani, H.; Pittman, C. U., Jr. *Carbon* **2004**, *42*, 2433.

(27) Park, S. H. P.; MaClain, S.; Tian, Z. R.; Suib, S. L.; Karwacki, C. *Chem. Mater.* **1997**, *9*, 176.

(28) Haydar, S.; Moreno-Castilla, C.; Ferro-Garcia; Carrasco-Marin, F.; Rivera-Utrilla, J.; Perrard; Joly, J. P. *Carbon* **2000**, *38*, 1297.

(29) Zhou, J. H.; Sui, Z. J.; Zhu, J.; Li, P.; Chen, D.; Dai, Y. C.; Yuan, W. K. *Carbon* **2007**, *45*, 785.

(30) Park, S. J.; Kim, B. J. *Mater. Sci. Eng., A* **2005**, *408*, 269.

(31) Figueiredo, J. L.; Pereira, M. F. R.; Freitas, M. M. A.; Orfao, J. J. M. *Carbon* **1999**, *37*, 1379.
(32) Defossse, C. In *Characterization Of Heterogeneous Catalysts*; Delannay F, Ed.; Marcel Dekker, Inc.: New York, 1984.
(33) Hall, P. J.; Calo, J. M. *Energy Fuels* **1989**, *3*, 370.
(34) Calo, J. M.; Cazorla-Amoros, D.; Linares-Solano, A.; Roman-Martinez, M. C.; Salinas-Martinez De Lecea, C. *Carbon* **1997**, *35*, 543.
(35) Marchon, B.; Carraza, J.; Heinemann, H.; Somorjai, G. A. *Carbon* **1988**, *28*, 507.
(36) Ago, H.; Kugler, T.; Cacialli, F.; Salaneck, W. R.; Shaffer, M. S. P.; Windle, A. H.; Friend, R. H. *J. Phys. Chem. B* **1999**, *103*, 8116.
(37) Mawhinney, D. B.; Naumenko, V.; Kuznetsova, A.; Yates, J. T.; Liu, J.; Smalley, R. E. *Chem. Phys. Lett.* **2000**, *324*, 213.
(38) Briggs, D.; Seah; M. P. *Practical Surface Analysis*; John Wiley & Sons Ltd.: U.K., 1994.

JP804413A